

High-gain observer-based model predictive control for cross tracking of underactuated autonomous Underwater Vehicles: A comparative study

Guangjie Zhang, Weisheng Yan, Jian Gao* & Changxin Liu

School of Marine Science and Technology, Northwestern Polytechnical University, Xi'an, China

*[E-mail: jiangao@nwpu.edu.cn]

Received 16 April 2017 ; revised 29 October 2017

In this paper, a disturbance observer-based model predictive control (DO-MPC) scheme is developed for cross tracking of underactuated autonomous underwater vehicles (AUVs) under sea current disturbances. A high-gain observer is used to estimate the current velocity, external sway force and yaw torque. Based on the disturbance estimates, a nonlinear model predictive controller is designed with consideration of actuator constraints. The control inputs are solved by optimizing the future trajectories of the nonlinear system under input constraints within a certain time horizon, which are predicted by the system model with estimated disturbances. The stability of the predictive control cross-tracking system is also proved with a Lyapunov-based method. The comparative simulation results with different algorithms are provided to validate the effectiveness of the proposed method.

[Keywords: autonomous underwater vehicle, high-gain observer, model predictive control, cross tracking, current disturbance]

Introduction

Autonomous underwater vehicles (AUVs) have been widely used to perform underwater missions, such as bottom survey, cable tracking¹, payload delivery, submerged wrecks detecting and mapping. Cross tracking refers to an AUV with any initial position and orientation to reach and follow a reference straight line which is generated by a geometric parameter but not by time². It is difficult to executed accurately due to the underactuated properties and actuator constraints of AUVs.

The tracking arrived problem has mostly been investigated in the past decades³. Peng and Wang⁴ proposed an output-feedback path-following control scheme for an underactuated AUV moving in a vertical plane. The unmeasured velocities were estimated by an extended state observer. The quadratic programming problem formulated from the desired guidance law optimization was solved by a projection neural network. Woolsey⁵ and Xiang⁶ both designed 3-D cross tracking

controllers for underactuated AUV considering the internal and external uncertainties. Xiang and Lapierre⁷ proposed a nonlinear controller to solve the nonlinear path following problem of a fully-actuated and under-actuated AUV respectively.

The aforementioned works mainly focused on the nonlinear tracking control of underactuated AUVs using Lyapunov stability theory, but the actuator constraints were not considered. Model predictive control (MPC) is a promising method to solve the constrained control problem, and it has been used for control of AUVs⁸⁻¹⁰. In this paper, MPC is employed to solve the constrained cross tracking control problem of an underactuated AUV. MPC performs online optimization of a cost function with respect to possible inputs based on the predictive model over a finite horizon. Compared with other control methods, MPC has many advantageous features such as the ability to handle system constraints directly¹¹⁻¹³ and to consider environmental disturbances and model

uncertainties^{14,15}.

MPC has been applied to various robotic systems because of its unique advantages in handling constraints. Oh and Sun¹⁶ used the line-of-sight (LOS) guidance method to solve the way-point tracking problems and improved the performance of the controller by solving the linear constrained optimization problem. Negenborn¹⁷ employed both the linear and nonlinear MPC algorithms for trajectory tracking control of ships. Considering the effects of external disturbances on the yaw angle, Li and Sun¹⁸ compared the disturbance compensated MPC algorithm with the conventional one under both constant and sinusoidal disturbances which were estimated by the difference between the measured and the calculated value using the linear model and the states at the previous step. However, the estimations of disturbances are sensitive to the measurement.

To solve this problem, several nonlinear disturbance observer algorithms¹⁹⁻²¹ were developed. Sariyildiz and Ohnishi¹⁹ designed a force control system based on a disturbance observer, and analyzed the robustness and stability of the system. Mohammadi and Tavakoli²⁰ designed a disturbance observer for robotic manipulators to deal with the constraints of the number of degrees-of-freedom (DOFs), the type of joints, and the control configuration. Su and Chen²¹ compared the time-domain and the frequency-domain disturbance observers, and presented a new functional disturbance observer (FDOB).

Among them, the high-gain observer is an effective observer and has been widely used in the nonlinear systems. Khalil and Praly²² designed a high-gain observer for nonlinear feedback control to estimate the unknown state feedback. Zhang and Zhou²³ used an initial high-gain observer for a class of nonlinear differential-algebraic equation subsystems, which made the observer errors converge to zero exponentially. Li and Kou et al.²⁴ proposed a high-gain observer for an engine dynamic model to improve the accuracy of pressure estimation and demonstrated the robustness and accuracy using the Laplace and Lyapunov method.

In this paper, the cross tracking control of underactuated AUVs with ocean current disturbances is investigated. Based on the nonlinear model of AUVs, the corresponding high-gain observer is employed to estimate the disturbances and the MPC with disturbance

compensation is used to stabilize the AUV to the desired linear trajectory.

Materials and Methods

Problem Formulation

The nonlinear cross tracking model of an underactuated AUV is depicted in Fig. 1¹⁷. The global coordinate system is established with the desired straight line as the x axis. O_b is the center of buoyance of the AUV, u_n is the surge velocity, e is the distance of the AUV to the desired line, and ψ is the yaw angle between the AUV heading and the x axis. The dynamics of surge is neglected, and the surge velocity is assumed as a constant. The torque N generated by the rudder is the control input.

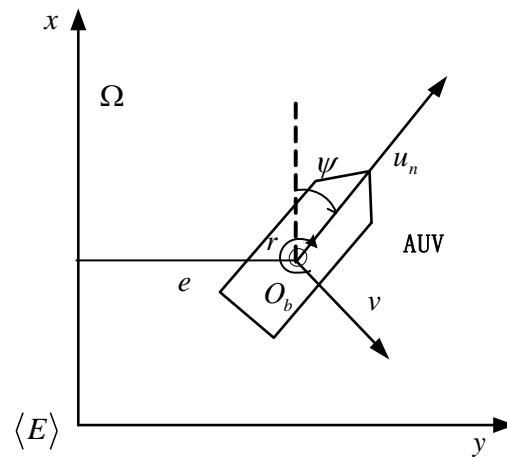


Fig. 1 – system modeling

The nonlinear model is given as follows²

$$\begin{aligned} \dot{e} &= u_n \sin \psi + v \cos \psi + \omega_1 \\ \dot{\psi} &= r \\ \dot{v} &= [d_{22}v - m_{11}u_n r] / m_{22} + \omega_3 \\ \dot{r} &= [-m_{22}u_n v + m_{11}u_n v + d_{33}r + N] / m_{33} + \omega_4 \end{aligned} \tag{1}$$

where $m_{11} = m - X_{\dot{u}}$, $m_{22} = m - Y_{\dot{v}}$, and $m_{33} = m - Z_{\dot{\omega}}$ are the inertia factors including the added mass, $d_{22} = Y_v$ and $d_{33} = N_r$ are damping coefficients, ω_1 is the current velocity, ω_3 is the external sway force, and ω_4 is the yaw moment disturbance.

The system model can be expressed in a compact form as:

$$\begin{aligned} \dot{x}(t) &= f(x(t), u(t)) + \omega \\ \dot{\omega} &= 0 \\ y(t) &= x(t) \end{aligned} \tag{2}$$

where $x = [e \ \psi \ v \ r]^T$, $u = N$, $\omega = [\omega_1, 0, \omega_3, \omega_4]$

The cross tracking control aims to drive the AUV to move along the given course defined by the x axis with the forward velocity u_n from any initial position.

High-gain Observer-based Model Predictive Cross Tracking Control

The nonlinear MPC close-loop control scheme with a high-gain disturbance observer is shown in Figure 2:

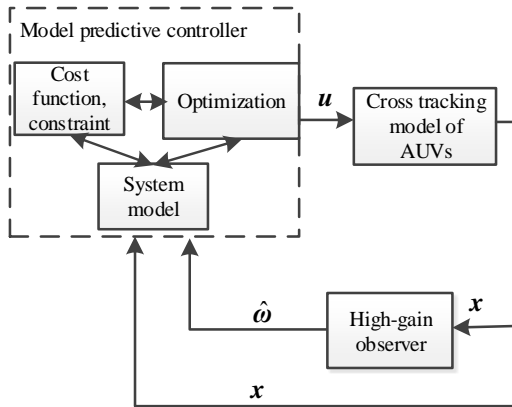


Fig. 2 – the proposed model predictive control system with disturbance observer

The architecture in Fig. 2 describes the main components of an AUV guidance system: the cross tracking model, the high-gain observer and the model predictive controller.

High-gain Disturbance Observer

A high-gain observer²² is designed as follows:

$$\begin{aligned}\dot{\hat{x}} &= \hat{f}(\hat{x}, u) + h_1(x - \hat{x}) \\ \dot{\hat{\omega}} &= 0 + h_2(x - \hat{x})\end{aligned}\quad (3)$$

where $\hat{f}(x, u)$ is the nominal system function.

The estimation errors of the state and disturbance are defined as

$$\begin{bmatrix} \tilde{x} \\ \tilde{\omega} \end{bmatrix} = \begin{bmatrix} x - \hat{x} \\ \omega - \hat{\omega} \end{bmatrix}\quad (4)$$

and the corresponding derivatives can be obtained as

$$\begin{aligned}\dot{\tilde{x}} &= \delta(x, \tilde{x}, u) + \omega + h_1\tilde{x} \\ \dot{\tilde{\omega}} &= -h_2\tilde{x}\end{aligned}\quad (5)$$

where

$$\delta(x, \tilde{x}, u) = f(x, u) - \hat{f}(\hat{x}, u)\quad (6)$$

Therefore, the following equations are obtained:

$$\begin{bmatrix} \dot{\tilde{x}} \\ \dot{\tilde{\omega}} \end{bmatrix} = \begin{bmatrix} -h_1 & 1 \\ -h_2 & 0 \end{bmatrix} \begin{bmatrix} \tilde{x} \\ \tilde{\omega} \end{bmatrix} + \begin{bmatrix} \delta \\ 0 \end{bmatrix}\quad (7)$$

Because of the existence of δ , h_1 and h_2 must be designed to reduce the effect of δ on \tilde{x} . The transfer function from δ to \tilde{x} is

$$G_0(s) = \frac{1}{s^2 + h_1s + h_2} \begin{bmatrix} 1 \\ s + h_1 \end{bmatrix}\quad (8)$$

The observer system is stable if h_1 and h_2 are both greater than 0. We must choose the most appropriate values of h_1 and h_2 to make the absolute value of $G_0(s)$ sufficiently small.

We can rewrite Eq. (8) as

$$G_0(s) = \frac{\frac{1}{\sqrt{h_2}}}{\left(\frac{s}{\sqrt{h_2}}\right)^2 + \frac{h_1}{\sqrt{h_2}}\frac{s}{\sqrt{h_2}} + 1} \begin{bmatrix} \frac{1}{\sqrt{h_2}} \\ \frac{h_1}{\sqrt{h_2}} + \frac{s}{\sqrt{h_2}} \end{bmatrix}\quad (9)$$

Define h_1, h_2 as

$$h_1 = \frac{\alpha_1}{\varepsilon}, \quad h_2 = \frac{\alpha_2}{\varepsilon^2}\quad (10)$$

where α_1, α_2 are positive constants and ε is arbitrarily small. Therefore, by choosing a small ε , the high gain observer can be designed more appropriately²².

Nonlinear Model Predictive Cross Tracking Control

MPC is an iterative optimization strategy. During each sampling instant k , it obtains the optimal input vector by minimizing a cost function subject to constraints based on the measured or estimated states. To facilitate the implementation of MPC, the original continuous model is firstly discretized as follows

$$\begin{aligned}\mathbf{x}(k+1) &= \mathbf{f}_d(\mathbf{x}(k), \mathbf{u}(k)) \\ \mathbf{y}(k) &= \mathbf{x}(k),\end{aligned}\quad (11)$$

where \mathbf{f}_d stands for the discretized system function. It is assumed that the length of control sequence is constant in the time period of $([(k-1)T_s, kT_s]) (k=1, 2, \dots, N_p)$. N_p is the prediction horizon, and T_s is the sampling interval.

Based on the current measured or estimated states, future predictions can be written as the functions of control sequence

$\mathbf{u}(k+i)$ ($i=0,1,\dots,N_p-1$). In step k , the simulation of future steps has a minimum linear tracking error:

$$\begin{aligned} & \min_{\bar{\mathbf{u}}(k)} J(\bar{\mathbf{x}}(k), \bar{\mathbf{u}}(k)) \\ J(\bar{\mathbf{x}}(k), \bar{\mathbf{u}}(k)) = & \\ & \sum_{i=1}^{N_p} (\bar{\mathbf{y}}(k+i|k) - \mathbf{y}_{ref})^T \mathbf{Q} (\bar{\mathbf{y}}(k+i|k) - \mathbf{y}_{ref}) \\ & + \sum_{i=0}^{N_p} \mathbf{u}(k+i|k)^T \mathbf{R} \mathbf{u}(k+i|k) \end{aligned} \tag{12}$$

s.t.

$$\mathbf{x}(k+i+1) = \mathbf{f}_d(\mathbf{x}(k+i), \mathbf{u}(k+i), \hat{\boldsymbol{\omega}}(k)) \tag{13}$$

$$\bar{\mathbf{y}}(k+i) = \mathbf{x}(k+i) \tag{14}$$

$$\mathbf{y}_{ref}(k) = [0 \ 0 \ 0 \ 0]^T \tag{15}$$

$$\mathbf{u}_{min} \leq \mathbf{u}(k+i) \leq \mathbf{u}_{max}, i=0,1,\dots,N_p-1 \tag{16}$$

where $\mathbf{x}(k)$ is the state matrix and $\bar{\mathbf{u}}(k)$ is the control input matrix. $\bar{\mathbf{y}}(k+i|k)$ stands for the predictive output vector at step $k+i$. \mathbf{Q} and \mathbf{R} are the weighting matrices of appropriate dimensions. We obtain a sequence of optimal results $\mathbf{u}(k|k), \mathbf{u}(k+1|k), \dots, \mathbf{u}(k+N_p-1|k)$ by solving the optimization problem Eq.(12)-(16), whose first element can be used as the optimal control input. In this way, the optimization problem can be recast as a quadratic programming problem¹⁸.

The DO-MPC algorithm can be summarized as follows¹⁶:

- (1) At step k , estimate the disturbance $\hat{\boldsymbol{\omega}}(k)$ using the high-gain observer.
- (2) Use the measured states $\mathbf{x}(k)$ together with $\hat{\boldsymbol{\omega}}(k)$ to obtain the future predicted outputs $\bar{\mathbf{y}}(k+i|k), i=1,\dots,N_p$ which is also a function of the future control inputs $\mathbf{u}(k+i|k), i=0,1,\dots,N_p-1$.
- (3) Solve the quadratic programming problem Eq.(12) (using MATLAB function *fmincon*) under the constraints and get the optimal control sequence $\mathbf{u}(k+i|k), i=0,1,\dots,N_p-1$.
- (4) Obtain the first element of the above optimal solution $\mathbf{u}(k|k)$ as the output of the controller, and it will be used as the input of the system model.
- (5) At next step $k+1$, return to step (1).

Stability Analysis

Optimality in some part of the time domain does not imply stability²⁵. We can see that the cost function of MPC is not defined in the infinite horizon, so it cannot guarantee that the minimum value of cost function decreases monotonically at each step. This section analyzes the stability of the MPC algorithm.

Theorem 1: The model predictive control system for cross tracking is stable when the terminal constraints X_f are close sets, and the terminal cost function $F(\mathbf{x}(k+N_p|k))$ is continuous-differential²⁶.

Proof: The cost function can be extended to the whole time domain:

$$\begin{aligned} \mathbf{J}(k) = & \sum_{i=0}^{N_p-1} g(\mathbf{x}(k+i|k), \mathbf{u}(k+i|k)) \\ & + F(\mathbf{x}(k+N_p|k)) \end{aligned} \tag{17}$$

where $g(\mathbf{x}(k), \mathbf{u}(k))$ is the stage cost at step k while

$F(\mathbf{x}(k+N_p|k)) = \sum_{i=N_p}^{\infty} g(\mathbf{x}(k+i|k), \mathbf{u}(k+i|k))$ is its cost function after step $k+N_p$. Obviously, the value of $F(\mathbf{x}(k+N_p|k))$ is not implemented in MPC but it affects the stability of the control system. It is assumed that the controller $\Phi(\mathbf{x})$ can ensure the system asymptotically stable when the system enters X_f .

At step k , the optimal control sequence is expressed as

$$\mathbf{U}^*(k) = \{\mathbf{u}^*(k|k), \dots, \mathbf{u}^*(k+N_p-1|k)\} \tag{18}$$

and its resultant optimal state trajectory is given by

$$\mathbf{X}^*(k) = \{\mathbf{x}^*(k+1|k), \dots, \mathbf{x}^*(k+N_p|k)\} \tag{19}$$

Then the minimized cost function at step k is

$$\begin{aligned} \mathbf{J}_p^* = & \sum_{i=0}^{N_p-1} g(\mathbf{x}^*(k+i|k), \mathbf{u}^*(k+i|k)) \\ & + F(\mathbf{x}^*(k+N_p|k)) \end{aligned} \tag{20}$$

At step $k+1$, the state quantity $\mathbf{x}^*(k+1|k)$ is controlled by the input quantity $\mathbf{u}^*(k|k)$. Then a feasible solution is

$$\mathbf{U}(k+1) = \{\mathbf{u}(k+1|k+1), \dots, \mathbf{u}(k+N_p|k+1)\} \tag{21}$$

where $\mathbf{u}(k+i|k+1) = \mathbf{u}^*(k+i|k)$ ($1 \leq i \leq N_p-1$),

$$\mathbf{u}(k+N_p|k+1) = \Phi(\mathbf{x}^*(k+N_p|k)).$$

Then its new state trajectory is

$$\mathbf{X}^*(k+1) = \{\mathbf{x}^*(k+2|k), \dots, \mathbf{x}^*(k+N_p+1|k)\} \quad (22)$$

The cost function is

$$\begin{aligned} J_p(k+1) = & \sum_{i=1}^{N_p} g(\mathbf{x}^*(k+i|k), \mathbf{u}^*(k+i|k)) \\ & + F(\mathbf{x}^*(k+N_p+1|k)) \end{aligned} \quad (23)$$

Therefore, we have

$$\begin{aligned} & \mathbf{J}_p^*(k) - \mathbf{J}_p(k+1) \\ & = g(\mathbf{x}^*(k|k), \mathbf{u}^*(k|k)) + F(\mathbf{x}^*(k+N_p|k)) \\ & \quad - g(\mathbf{x}^*(k+N_p|k), \mathbf{u}^*(k+N_p|k)) \\ & \quad - F(\mathbf{x}^*(k+N_p+1|k)) \\ & = g(\mathbf{x}^*(k|k), \mathbf{u}^*(k|k)) \geq 0 \end{aligned} \quad (24)$$

which means $\mathbf{J}_p(k+1) \leq \mathbf{J}_p^*(k)$. In addition, $\mathbf{U}(k+1)$ is a feasible solution of step $k+1$, and $\mathbf{U}^*(k+1)$ is the optimal solution. Therefore, we have

$$\mathbf{J}_p^*(k+1) \leq \mathbf{J}_p(k+1) \leq \mathbf{J}_p^*(k) \quad (25)$$

In summary, the MPC control strategy is asymptotically stable.

Because the control inputs and system states are under constraints, the system may not reach the terminal constraint set X_f within its prediction horizon. Assuming that the state $\mathbf{x}(k)$ of the step m reaches the terminal constraints X_f , the cost function after step $k+N_p$ can be written as follows:

$$\begin{aligned} F(\mathbf{x}(k+N_p|k)) = & \sum_{i=N_p}^{m-1} g(\mathbf{x}(k+i|k), \mathbf{u}(k+i|k)) \\ & + F(\mathbf{x}(k+m|k)) \end{aligned} \quad (26)$$

Then the stability of the proposed system under the constraints X_f can also be shown in Eq.(26) similarly to Eq.(17). In conclusion, the stability of the proposed cross tracking system is proved.

Result and Discussion

In this paper, the model parameters of the REMUS AUV²⁷ are shown in Table 1:

parameter	value	parameter	value
m (kg)	30.5	g (N/kg)	9.81
Y_v (kg)	-35.5	$Z_{\dot{w}}$ (kg)	-35.5
N_r (kg·m ² /s)	-188	$X_{\dot{u}}$ (kg)	-0.930
Y_v (kg/s)	-262		

In order to validate the effectiveness of the high-gain observer, the conventional MPC without disturbance estimation is utilized to compare with the proposed method. In the simulation, the parameters are assumed as follows:

The initial state $\mathbf{x}_0 = [10 \ \pi/6 \ 0 \ 0]^T$;

The initial value of input $u(0) = 0$;

The forward velocity $u_n = 2.5$ m/s;

The desired output $\mathbf{y} = [0 \ 0 \ 0 \ 0]^T$;

The input constraint $|M| \leq 6.15u_n^2\delta$, $\delta = 15^\circ$;

The control horizon $N_c = 10$, the prediction horizon $N_p = 10$.

Disturbance Observer-based Model Predictive Cross Tracking Control

The constant sea current is assumed as $\boldsymbol{\omega} = [0.1 \ 0 \ 0.4 \ 0]^T$.

The simulation results are plotted as follows:

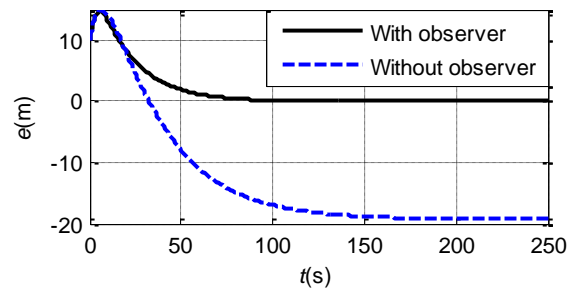


Fig. 3 – cross tracking errors of the AUV

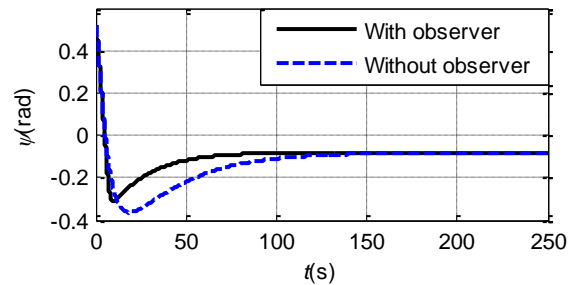


Fig. 4 – yaw angles between AUV and desired line

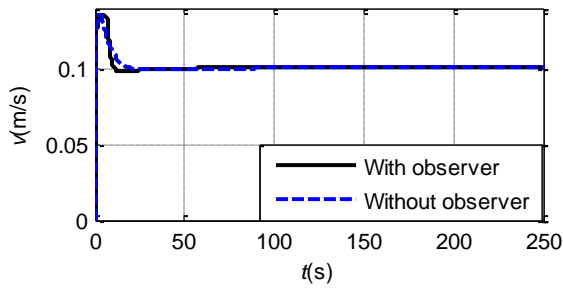


Fig.5 – sway velocities

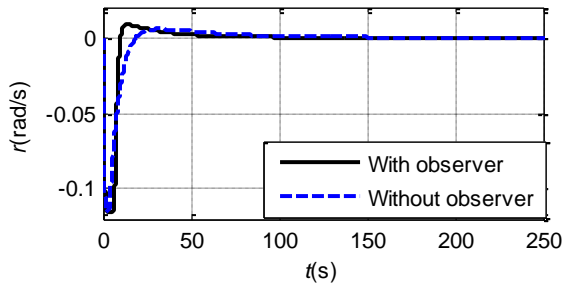


Fig.6 – yaw rates

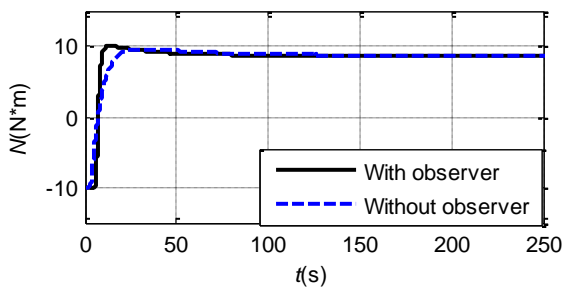


Fig.7 – control torques

In Fig. 3 and Fig. 5, it can be observed that without the estimation of disturbance, the simulation result is that the AUV runs along the parallel straight line 19 m away from the desired trajectory at a forward velocity of 2.5 m/s and a sway velocity of 0.1 m/s. However, with the proposed high-gain observer-based MPC, the AUV finally arrives and moves along the desired trajectory with constant forward velocity and sway velocity. From Fig. 4, Fig. 6 and Fig. 7, we can see that there are also other parameters in common such as the yaw angle is -0.08 rad, the yaw rate is 0 and the input torque is 8.7 N/m.

No matter whether the disturbance observer is used or not, the system can reach the equilibrium state and the direction of the total velocity is the same as the desired line. The controller without observer cannot gain any information of disturbance, so the impacts of disturbance are reflected directly. However, in the proposed scheme, the observer estimates the disturbance accurately. Thus, the controller can eliminate it and the system can reach the desired states precisely.

Comparison between LMPC and NMPC

By assuming $\sin \psi \approx 0$ and $\cos \psi \approx 1$, we can obtain the linearized model¹⁵:

$$\begin{aligned} \mathbf{x}(k+1) &= \mathbf{A}_0 \mathbf{x}(k) + \mathbf{B}_0 \mathbf{u}(k) \\ \mathbf{y}(k) &= \mathbf{x}(k) \end{aligned} \tag{27}$$

$$\mathbf{A}_0 = \begin{bmatrix} 1 & u_n T_s & 1 & 0 \\ 0 & 1 & 0 & 1 \\ 0 & 0 & 1 + d_{22} / m_{22} T_s & -m_{11} u_n / m_{22} T_s \\ 0 & 0 & (m_{22} - m_{11}) u_n / m_{33} T_s & 1 + d_{33} / m_{33} T_s \end{bmatrix} \tag{28}$$

$$\mathbf{B}_0 = \begin{bmatrix} 0 \\ 0 \\ 0 \\ 1 / m_{33} T_s \end{bmatrix} \tag{29}$$

By replacing the nonlinear predict model to the linear one, we have the linear MPC (LMPC).

Under the constant disturbance above, LMPC and nonlinear MPC (NMPC) are used to realize the linear tracking control, respectively. Here are the comparisons:

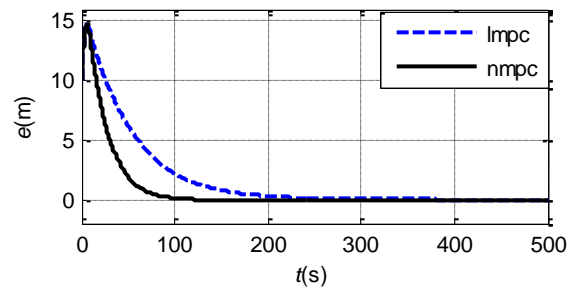


Fig.8 – cross-track errors of the AUV

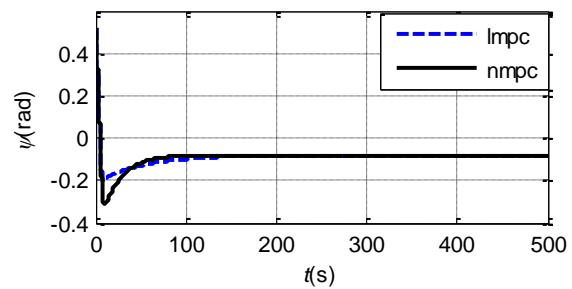


Fig.9 – yaw angles between AUV and desired line

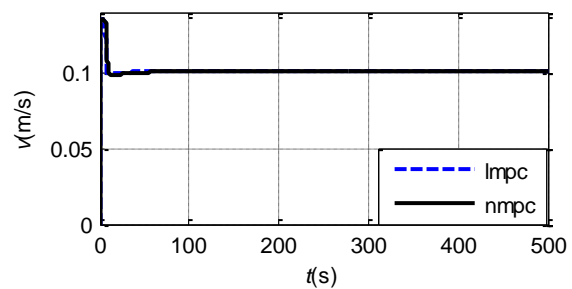


Fig.10 - sway velocities

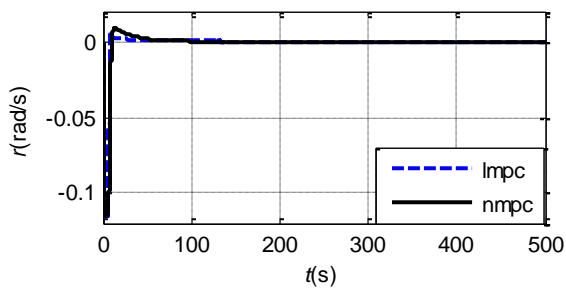


Fig.11 - yaw rates

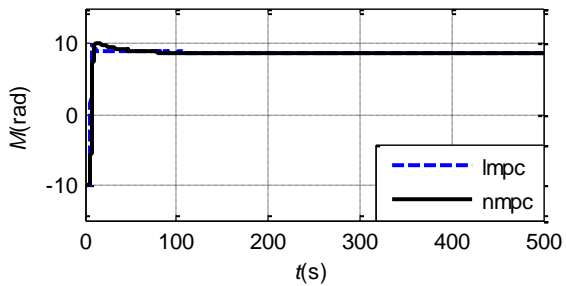


Fig.12 - control torques

We can draw a conclusion that there are different performances of NMPC and LMPC under the same condition. We believe that the system is stable when the distance error reaches the 5% error bound and keeps in the bound. From the figures above, the system reaches stability at 110 s under NMPC while it is 220 s under LMPC in Fig. 8. Before reaching stability, the torque M under NMPC has larger overshoot than it under LMPC, so it has larger yaw angle, which leads the AUV reaches the desired line faster.

Due to the nonlinearity of the considered system, the linear model is approximated from the real system when $\psi = 0$, so the error is getting larger with the increase of ψ . We may conclude that NMPC and LMPC both can complete the cross tracking control and both are stable. However, the NMPC outperforms for its faster convergence rate.

In summary, the high-gain observer can estimate the constant disturbances exactly, and the high-gain observer-based model predictive controller can ensure the stability and accuracy of the cross tracking control system. Both the LMPC and the NMPC meet the requirements, while NMPC achieves better performances.

Conclusion

In this paper, a high-gain observer-based model predictive control algorithm is proposed for the cross tracking control system of AUV. Considering the problem of ocean current, a high-gain observer is designed to estimate the

disturbance, and a model predictive controller is utilized based on the value of disturbance estimation and the measure states. By comparing the simulation results with and without the observer, the effectiveness of the high-gain observer is validated. And according to the simulation results of NMPC and LMPC, we conclude that NMPC has better performances than LMPC. In the future research, the proposed scheme will be extended to the 3D cross tracking control of an underactuated AUV.

Acknowledgment

This work is supported in part by the National Natural Science Foundation of China under the Grants of 61733014, 51579210, and 61633002, and in part by the Fundamental Research Funds for the Central Universities under the Grant of 3102017gx06001.

References

- 1 Xiang X., Yu C., Niu Z., et al., Subsea Cable Tracking by Autonomous Underwater Vehicle with Magnetic Sensing Guidance. *Sensors*, 2016, 16(8): 1-22.
- 2 Fossen T. I., *Marine Control Systems: Guidance, Navigation, and Control of Ships, Rigs and Underwater Vehicles*. Chichester, UK; New York, NY, USA; Brisbane, Australia; Toronto, Canada; Singapore: John Wiley & Sons Inc., 2005.
- 3 Shi Y., Shen C., Fang H., et al., Advanced Control in Marine Mechatronic Systems: A Survey. *IEEE/ASME Trans. Mechatron.*, 2017, 22(3): 1121-1131.
- 4 Peng Z., Wang J., Output-Feedback Path-Following Control of Autonomous Underwater Vehicles Based on an Extended State Observer and Projection Neural Networks (in press). *IEEE Trans. Syst. Man Cybern., Syst.*, 2017, 1-10.
- 5 Woolsey C. A., Techy L., Cross-track control of a slender, underactuated AUV using potential shaping. *Ocean Eng.*, 2009, 36(1): 82-91.
- 6 Xiang X., Yu C., Zhang Q., Robust fuzzy 3D path following for autonomous underwater vehicle subject to uncertainties. *Comput. Oper. Res.*, 2016, 84:165-177.
- 7 Xiang X., Lapierre L., Jouvencel B., Smooth transition of AUV motion control: From fully-actuated to under-actuated configuration. *Robot. Auton. Syst.*, 2015, 67:14-22.
- 8 Gao J., Liu C., Proctor A., Nonlinear model predictive dynamic positioning control of an underwater vehicle with an onboard USBL system. *J. Ma. Sci. Tech.-Japan*, 2016, 21(1): 57-69.
- 9 Gao J., Proctor A. A., Shi Y., et al., Hierarchical Model Predictive Image-Based Visual Servoing of Underwater Vehicles With Adaptive Neural Network Dynamic Control. *IEEE Trans. Cybernetics*, 2016, 46(10): 2323-2334.
- 10 Shen C., Shi Y., Buckham B., Integrated Path Planning and Tracking Control of an AUV: A Unified Receding Horizon Optimization Approach. *IEEE/ASME Trans. Mechatron.*, 2017, 22(3): 1163-1173.
- 11 Trodden P., Richards A., Cooperative distributed MPC of linear systems with coupled constraints. *Automatica*, 2013, 49(2): 479-487.

- 12 Brunner F. D., Heemels M., Allgöwer F., Robust self-triggered MPC for constrained linear systems: A tube-based approach. *Automatica*, 2016, 72:73-83.
- 13 Ismail Z. H., Mokhar M., Adaptive tracking control scheme for an autonomous underwater vehicle subject to a union of boundaries. *Indian J. Geo-Mar. Sci.*, 2013, 42(8): 999-1005.
- 14 Mohd-Mokhtar R., Aziz M., Arshad M. R., et al., Model identification and control analysis for underwater thruster system. *Indian J. Geo-Mar. Sci.*, 2013, 42(8): 992-998.
- 15 Anavatti S. G., Adaptive fuzzy control of unmanned underwater vehicles. *Indian J. Geo-Mar. Sci.*, 2011, 40(2): 168-175.
- 16 Oh S. R., Sun J., Path following of underactuated marine surface vessels using line-of-sight based model predictive control. *Ocean Eng.*, 2010, 37(2-3): 289-295.
- 17 Mohd-Mokhtar R., Aziz M., Arshad M. R., et al., Model identification and control analysis for underwater thruster system. 2014,
- 18 Li Z., Sun J., Disturbance Compensating Model Predictive Control With Application to Ship Heading Control. *IEEE Trans. Control Syst. Tech.*, 2011, 20(1): 257-265.
- 19 Sariyildiz E., Ohnishi K., On the Explicit Robust Force Control via Disturbance Observer. *IEEE Trans. Ind. Electron.*, 2015, 62(3): 1581-1589.
- 20 Mohammadi A., Tavakoli M., Marquez H. J., et al., Nonlinear disturbance observer design for robotic manipulators. *Control Eng. Pract.*, 2013, 21(3): 253-267.
- 21 Su J., Chen W. H., Yang J., On Relationship between Time-Domain and Frequency-Domain Disturbance Observers and Its Applications. *J. Dyn. Syst.*, 2016, 9(138).
- 22 Khalil H. K., High-gain observers in nonlinear feedback control. *Int. J. Robust Nonlin.*, 2013, 24(6): 993-1015.
- 23 Zhang Q., Zhou Y., Hu K., Initialized high gain observer for a class of Nonlinear Differential- Algebraic Equation Subsystems. 2012,
- 24 Li Y., Kou X., Zheng T., Transportation-cyber-physical-systems-oriented engine cylinder pressure estimation using high gain observer. *Chinese Phys. B*, 2015, 24(5): 058901-058907.
- 25 Kaiman R. E., Contributions to the Theory of Optimal Control. *Bol. Soc. Mat. Mexicana*, 1960, 5(63): 102-119.
- 26 Li X., Liu S., Tan K. K., et al., New model predictive control for improved disturbance rejection. 2016, 4318-4323.
- 27 Taleshian T., Minagar S., Motion planning for an autonomous underwater vehicle. 2015, 285-290